Journal of Fluids and Structures (2002) **16**(8), 1111–1126
doi:10.1006/jfls.2002.0466.available online at http://www.idealibrary.com on IDEAL®

AEROELASTICITY ANALYSIS OF AN INDUSTRIAL GAS TURBINE COMBUSTOR USING A SIMPLIFIED COMBUSTION MODEL

C. Bréard, A.I. Sayma, M. Vahdati and M. Imregun

Centre of Vibration Engineering, Mechanical Engineering Department, Imperial College of Science Technology and Medicine London SW7 2BX, U.K.

(Received 7 March 2001; and in final form 16 December 2001)

Lean premixed industrial gas turbine combustors are susceptible to flame instabilities, resulting in large unsteady pressure waves that may cause the discharge nozzle to experience excessive vibration levels. A detailed aeroelasticity analysis, aimed at investigating possible structural failure mechanisms, was undertaken using a time-accurate unsteady flow representation, a simplified combustion disturbance and a structural model of the discharge nozzle. The computational domain included the lower part of the combustor geometry as well as the nozzle guide vanes (NGVs) at the HP turbine inlet. A pressure perturbation, representing the unsteadiness due to the combustion process, was applied below the tertiary fuel inlet and its frequency was set to each structural natural frequency in turn. The propagation of the pressure perturbation through the combustor nozzle, its reflection from the NGVs and further reflections were monitored using two different models. The first one, the so-called "open" system, ignored the reflections from the upper part of the combustion chamber while the second one, the "closed" system, assumed full reflection with an appropriate time shift. The calculations have shown that the imposed excitation could generate unsteady pressure shapes that were correlated with the "flap" modes of the discharge nozzle. In addition, an acoustic resonance condition was observed when the forcing pressure wave had a frequency close to 550 Hz, the experimentally observed failure frequency of the nozzle. The co-existence of these two factors, i.e., excitation/structural-mode match and the possibility of acoustic resonance, was thought to have the potential of producing very high vibration response.

1. INTRODUCTION

Increasingly stringent legislative requirements to reduce NO_x, CO and soot emission levels from industrial gas turbines have led to lower combustion temperatures by means of lean premixing. However, such modes of combustion may become prone to flame instability, the excitation from which may yield excessive noise and cause structural failure. Indeed, the sound waves, generated by the unsteady heat release, may produce large pressure and velocity fluctuations in the core volume of the combustor. If the flame oscillation and the ensuing fluctuations are in phase, the resulting thermoacoustic interactions can yield high-amplitude acoustic waves which are of great concern to designers. The situation is further complicated by the actual geometry of the combustor, the temperature distribution and surface reflectivity because of the possible wave reflections (Hubbard & Dowling 2000). The detailed modelling of self-excited combustor

0889-9746/02/081111 + 16 $35.00/0

oscillations remains a great challenge, though significant progress has been made in recent years (Smith & Leonard 1997; Brookes *et al.* 1999, 2000; Zhu *et al.* 2000)

From the outset, it must be stressed that the purpose of this paper is not to model the combustion instabilities but to study the effect of the resulting acoustic waves on structural vibration by using an integrated aeroelasticity model. It is proposed to use a typical industrial gas turbine combustor which has been the subject of many previous studies. The CFD analysis of the complete geometry, including premixing ducts, the fuel injectors and the discharge nozzle, was undertaken by Birkby *et al.* (2000) to study the operation of the combustor. A modified k–epsilon model was coupled to a laminar flamelet combustion model in order to obtain a realistic turbulent burning rate representation. Here attention is focused on the discharge nozzle part of the combustor as this component is known to be prone to failure because of excessive structural response at around 550 Hz. As mentioned earlier, the excitation is due to thermoacoustic coupling arising from the flame instability in lean premixed combustion. The aim is to investigate the susceptibility of the structural modes to such excitation with a view to minimize the vibration levels by modifying the design of the discharge nozzle. For a resonant condition, the unsteady pressure fluctuations must match, both in frequency and shape, the modes of vibration. Since the geometry of the combustor determines not only the propagation and reflection of the unsteady pressure waves (i.e., the excitation) but also the natural frequencies and mode shapes of the structure (i.e., the response), such an analysis needs to be conducted with an integrated fluid–structure model where the structural flexibility and the flow unsteadiness are considered together (Sayma *et al.* 2000*a*). A more comprehensive investigation of the problem would need to have included a more representative combustion model (Birkby *et al.* 2000), so that flame oscillation and structural vibration could be coupled directly through the pressure fluctuations. Here, the flame oscillation will be represented by an unsteady pressure perturbation imposed at a plane just under the tertiary fuel inlet. Such a simple model ignores the possibility of the flame being perturbed further by the unsteady pressure waves. However, since the amplitude and frequency of the perturbation are chosen in the light of available experimental data, the simplified representation is expected to be adequate for the purposes of linking structural response and combustion unsteadiness.

The objectives of the current study are twofold, as follows:

(i) To assess if the imposed pressure perturbation, i.e., the simplified flame oscillation model, will excite specific structural modes. In this case, the frequency of the perturbation will be set to each structural natural frequency in turn.
(ii) To monitor the amplitude variation of the unsteady pressure due to the imposed perturbation. The frequency of the perturbation will be varied within the 300–750 Hz frequency range to investigate the possibility of acoustic resonance near the observed maximum response frequency of 550 Hz.

2. OVERVIEW OF THE AEROELASTICITY METHODOLOGY

The details of the unsteady flow and aeroelasticity code that will be used in this study have already been described by Vahdati & Imregun (1996) and Sayma *et al.* (2000*a*, *b*) and will not be repeated here. However, for the sake of completeness, an overview of the aeroelasticity modelling methodology is given in what follows.

The flow domain is described using general unstructured grids of 3-D elements such as tetrahedra, hexahedra and wedges, a feature that offers great flexibility for modelling

complex shapes. The individual elements can have any number of boundary faces and the flow variables are stored at the vertices. The numerical scheme is second-order accurate in space for tetrahedral meshes. For prismatic and hexahedral cells, the scheme is still second-order accurate for regular cells with right angles. In the worst case of a highly skewed cell, the scheme will reduce to first-order accuracy. However, hexahedral meshes are usually generated in the boundary layer where orthogonality results in regular cells. Similarly, prismatic cells are usually generated in a structured manner by projecting triangular meshes on radial layers and then connecting them. Highly skewed meshes are unlikely to occur in these situations.

The computational domain is stored using an edge-based date structure which results in a central difference scheme for the advection terms which is stabilized using a mixture of second- and fourth-order matrix artificial dissipation. The time stepping is done in an implicit fashion and hence very large CFL numbers can be used without creating numerical instabilities in the solution algorithm. The so-called "dual time stepping" procedure is used for unsteady calculations. The time accuracy is guaranteed by the outer iteration level where the time step is fixed throughout the solution domain, while the inner iterations can be performed using traditional acceleration techniques such as local time stepping and residual smoothing. The code can be run in viscous mode via Reynolds-averaged Navier–Stokes equations with Baldwin–Barth, Spalart–Allmaras or q–zeta turbulence models.

The structural model is based on a linear modal model, the mode shapes and natural frequencies being obtained via standard FE analysis techniques. The mode shapes are interpolated from the structural mesh onto the aerodynamic mesh as the two discretization levels are unlikely to be coincident. Boundary conditions from the structural and aerodynamic domains are exchanged at each time step and the aeroelastic mesh is moved to follow the structural motion using a spring analogy algorithm. A typical solution cycle at some arbitrary time step is shown in Figure 1.

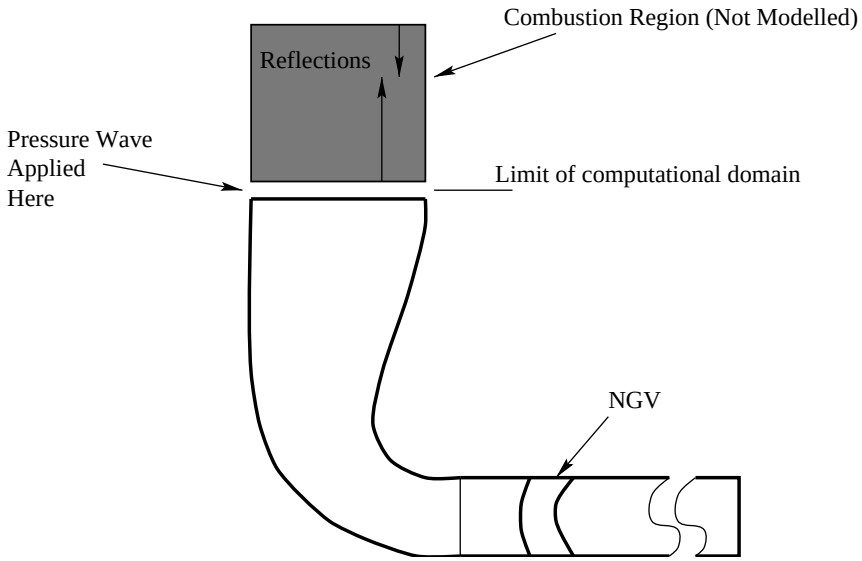

Figure 1. Procedure for time-accurate aeroelasticity computations.

3. STEADY STATE FLOW COMPUTATIONS

The flow is known to be choked at the discharge nozzle exit, a feature that needs to be represented in the numerical model. This condition has been achieved by including the nozzle guide vanes (NGVs) of the HP turbine to obtain the correct flow exit conditions (Figure 2). Such an approach was found to yield better results than imposing representative boundary conditions at the discharge nozzle exit. Because of the cyclic symmetry, five NGVs were used in the numerical model. The mixed-element mesh of the computational domain is shown in Figure 3. A fully unstructured grid of tetrahedra was

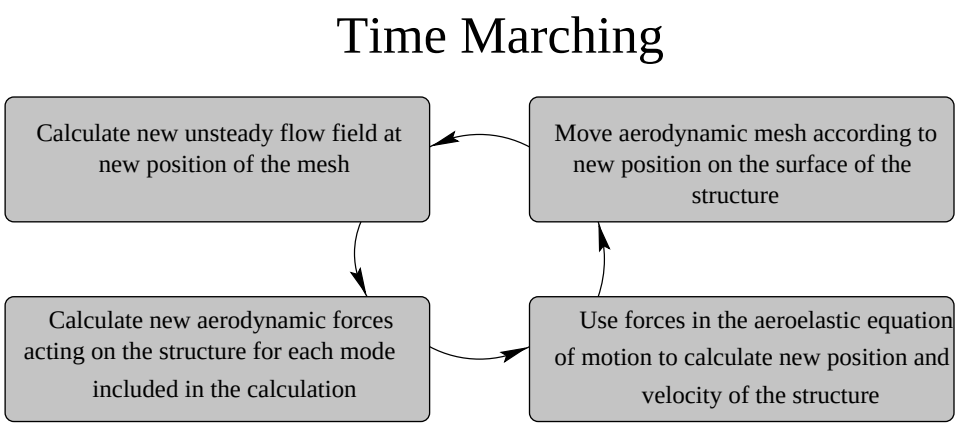

Figure 2. Schematic representation of the computational domain (not to scale). NGV: Nozzle guide vane.

Figure 3. Computational mesh.

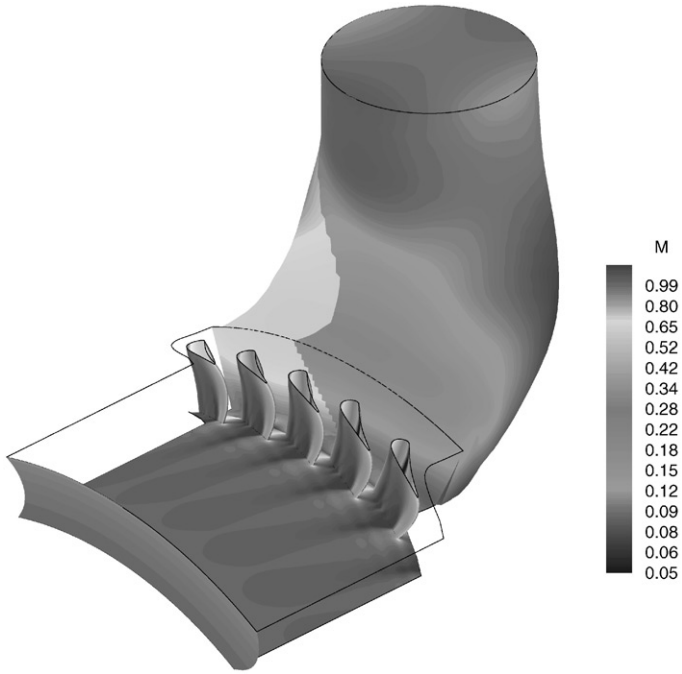

Figure 4. Steady state Mach number contours.

used to discretize the discharge nozzle itself, whilst a semi-structured mesh was used for the five NGVs (Sbardella *et al*. 2000).

Since the main focus of this study is wave propagation, which is primarily an inviscid phenomenon, the flow was modelled using the Euler equations. The gas in the combustor was treated as calorically perfect, with a specific heat ratio of 1·3475 and a specific heat of $= 1129{\cdot}8\,\mathrm{J/kg/K}$. The inlet boundary conditions were specified for the following quantities: the mass flow through the discharge nozzle, the total pressure and the total temperature. The inlet flow was assumed to be uniform with zero swirl. The exit pressure and temperature were specified downstream of the NGVs. Figure 4 shows the Mach number contours of the steady flow through the discharge nozzle. The flow accelerates slowly through the discharge nozzle as the area reduces towards the exit plane and reaches sonic conditions at the NGV exit. The region of supersonic flow is curtailed by a shock wave, a feature which can be seen more clearly from the steady state pressure contours of Figure 5. The presence of such a flow condition will prevent downstream disturbances from reaching the core volume of the combustor.

4. STRUCTURAL MODEL OF THE DISCHARGE NOZZLE

The vibration modes of the discharge nozzle, the main of area of interest because of structural failures, were obtained from a standard finite element model. The resulting modal model was used in the unsteady flow computations with moving meshes to accommodate structural motion. Interest was confined to the 200–1000 Hz frequency range and, as shown in Figure 6, eight modes were identified. An inspection of Figure 6 indicates that the vibration modes can be classified as ''flap'' or ''flex''. The flap modes, occurring at 328, 443, 556, 782 and 934 Hz, have their maximum deflection on the

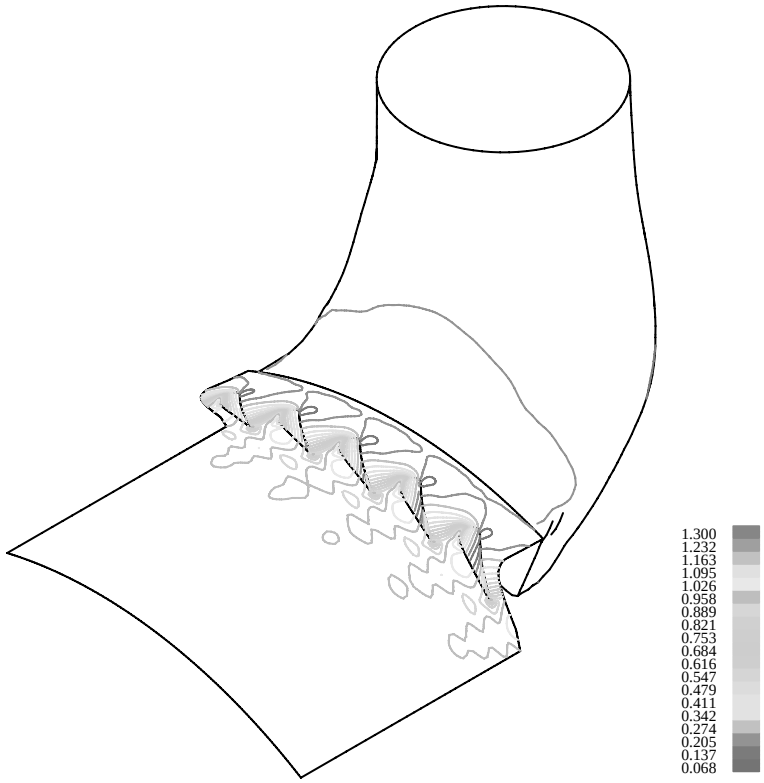

Figure 5. Steady state pressure contours.

centre-line of the nozzle. On the other hand, maximum displacements are reached off the centre-line for the flex modes which occur at 278, 640 and 739 Hz.

5. OVERVIEW OF THE AEROELASTICITY CALCULATIONS

The unsteady computations were initiated from the steady state solution of the previous section by imposing a sinusoidally varying pressure perturbation in order to simulate the disturbance caused by the pulsating combustion front (Fig 2). The amplitude of the perturbation was set to 0·3% of the ambient pressure as such a value was believed to be representative of the combustion disturbances. As mentioned earlier, the frequency of the perturbation was varied according to the objectives of the analysis. The imposed pressure perturbation, termed the ''forward running wave'' propagates downstream inside the nozzle but it is reflected back upstream by the NGVs, the reflected wave being termed the ''backward running wave''. The unsteady computations were conducted in two phases, each dealing with the backward running wave in a different manner.

The first set of calculations, corresponding to the so-called ''open system'', allowed the backward running waves to pass through the upper boundary but further reflections from the combustion area and the upper surface of the combustor were ignored. The second set of computations, conducted for the ''closed system'', included the reflection of the backward running waves from the upper surface of the combustor. The backward running waves exiting the upper computational boundary were fed back to the computational domain with a suitable time lag which was determined using the distance between the

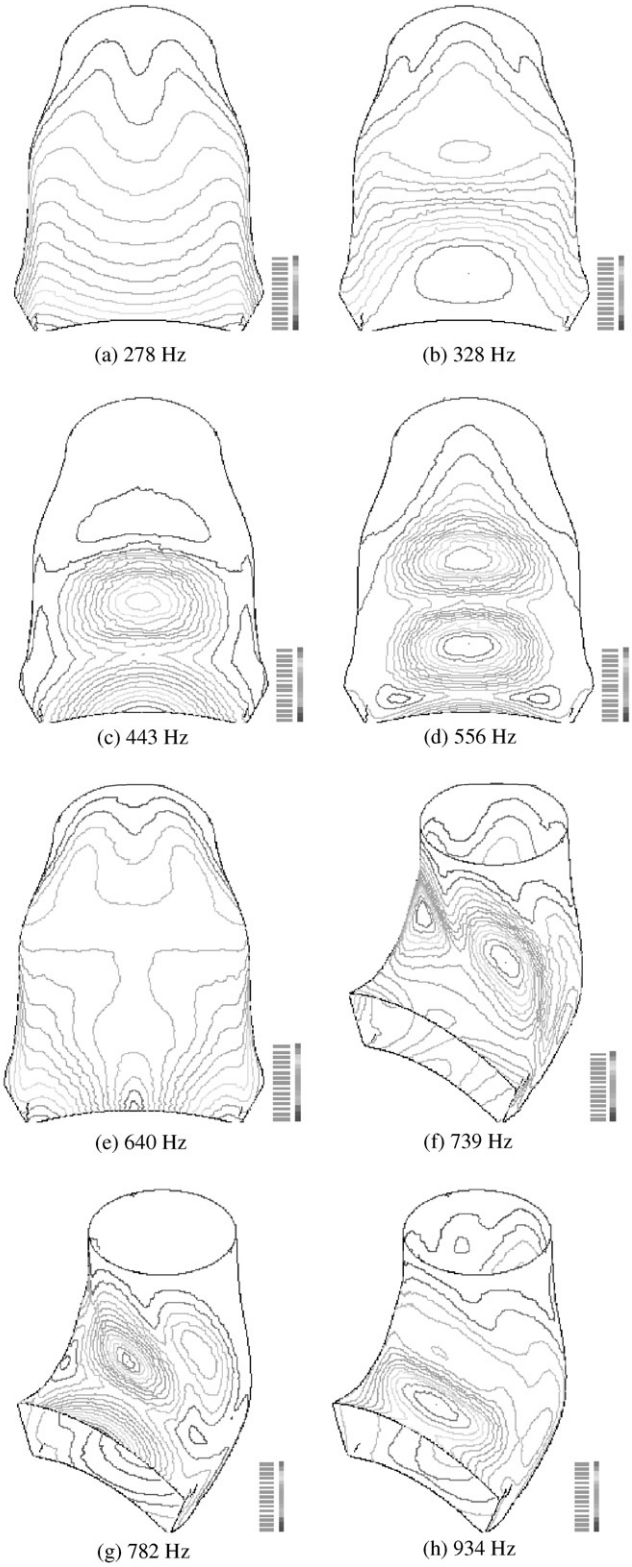

Figure 6. Vibration modes of the discharge nozzle.

computational boundary and the upper surface of the combustor. The reflection was assumed to be perfect, and any attenuation/reflection due to the combustion process was ignored. It was further assumed that the speed of sound remained constant in the combustion area when calculating the time lag. The main objective of the open system calculations is to study if the vibration modes will be excited by the downstream-propagating unsteady pressure shape created by the input perturbation representing the combustion instability. The aim of the closed system calculations is to assess if the amplitude of the unsteady pressure is likely to grow due to the superposition of forward and backward running waves, a situation that can broadly be described as acoustic resonance. The two sets of calculations, which include the structural motion of the discharge nozzle, will now be described in more detail.

6. "OPEN SYSTEM" CALCULATIONS

The frequency of the inlet pressure perturbation was set to the first five natural frequencies of the discharge nozzle in turn and the modal forces amplitudes, corresponding to each excitation case are plotted in Figure 7. The modal force, defined as the scalar product of the unsteady pressure vector and the structural mode shape vector, indicates the contribution of the unsteady aerodynamic load vector to a given vibration mode. For instance, for an oscillating rigid aerofoil, the modal force can be considered as the unsteady lift force corresponding to rigid body motion. An inspection of Figure 7 reveals that the mode at 328 Hz will contribute to the response at all five excitation frequencies. Other significant modes include those at 934, 443, 556 and 782 Hz, all being previously identified as "flap" modes. No modal force is produced by any of the flex modes, a feature that indicates that those will be absent from the vibration response. The displacement amplitudes, where the contribution of each individual vibration mode is shown explicitly, are plotted in Fig. 8 for the same five excitation cases. As expected, the response is in the flap modes only, the highest responses being associated with the 328 and 556 Hz modes. Excitation cases 640 and 739 Hz, corresponding to flex and flexural mode frequencies, produce very low response. The response in the flap modes is likely to be due to a match

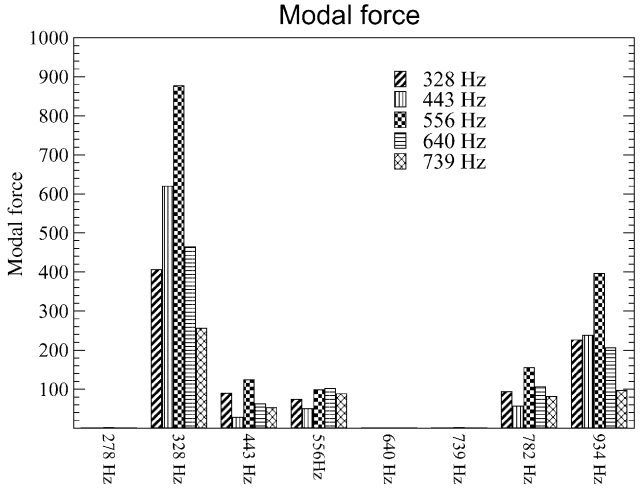

Figure 7. Amplitude of the modal force at various excitation frequencies.

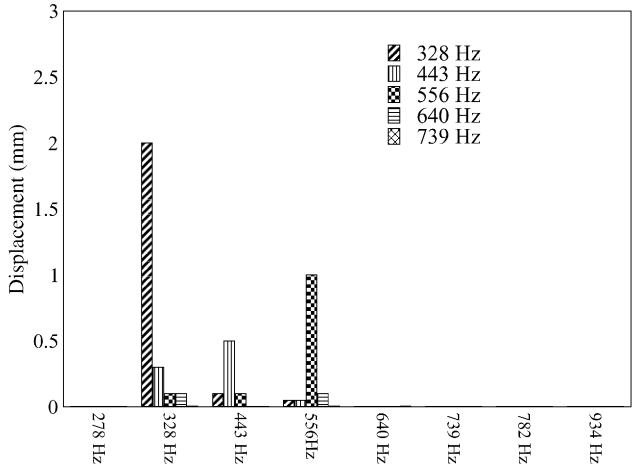

Figure 8. Amplitude of the displacement at various excitation frequencies.

between the unsteady pressure shape and the structural mode shapes while the lack of response in the flex modes can be explained by a mismatch. A more systematic correlation between such quantities can be performed by using the modal assurance criterion (MAC) of Allemang & Brown (1982). The correlation between two given vectors, ϕ_{UP} and ϕ_{ST}, can be expressed as

$$\mathrm{MAC} = \frac{|\phi_{UP}^{T}\phi_{ST}|^2}{(\phi_{UP}^{T}\phi_{UP})(\phi_{ST}^{T}\phi_{ST})} \tag{1}$$

where subscripts UP and ST denote unsteady pressure and structural mode shape, respectively. A MAC value of 0 indicates no correlation, while a MAC value of 1 indicates 100% correlation. Here we have eight structural modes and five unsteady pressure shapes, each corresponding to a fixed-frequency excitation of the open system. A 5×8 MAC matrix can thus be obtained by applying relationship (1) to all possible vector pairings. However, it is probably more instructive to consider the x, y and z directions separately by resolving the unsteady pressure and mode shape data using the surface normals at each point. Three MAC matrices were formed by adopting such an approach and the results are plotted in Figure 9. It can be seen that the second structural mode (328 Hz) is well correlated with the unsteady pressure shape for all three coordinate directions. Some further flap modes are also correlated but none of the flex modes are.

As can be seen from Figure 7, the maximum modal forces are obtained for excitation cases, 443 and 556 Hz, suggesting that the largest unsteady pressure fluctuations will occur between these two frequencies. Such an observation highlights the likelihood of an acoustic resonance in this range. In order to investigate this possibility further, additional open system computations were performed at 480, 500 and 580 Hz. The maximum value of the nozzle unsteady pressure p'_{max} as a function of the excitation frequency is plotted in Figure 10. There is a well defined peak at around 500 Hz, the imposed inlet combustion disturbance of 0·3% being amplified to 1·9%, or by a factor of 6·3. Clearly, such an amplification could yield excessive structural loads if the combustion disturbances were large, or if the forward and backward running waves were to superpose in an additive manner. This latter possibility will be investigated in the next section for the closed system.

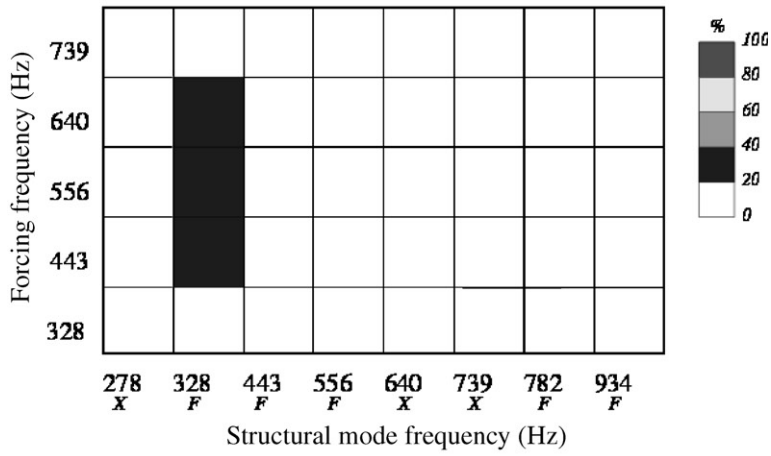

(a) x - direction

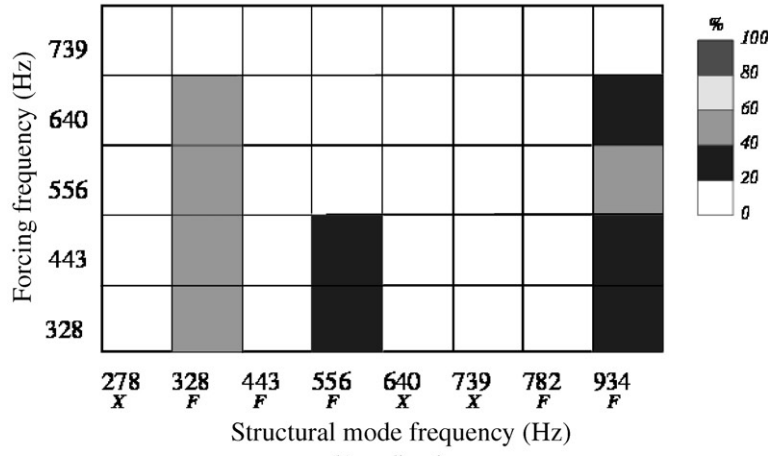

(b) y - direction

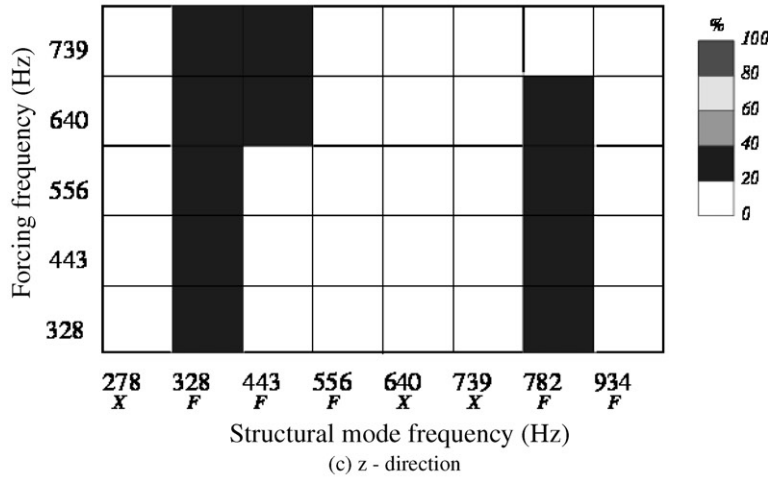

(c) z - direction

Figure 9. MAC correlation between unsteady pressure shapes and structural mode shapes : (a) in x-direction; (b) in y-direction; (c) in z-direction. X: flex mode, F: flap mode.

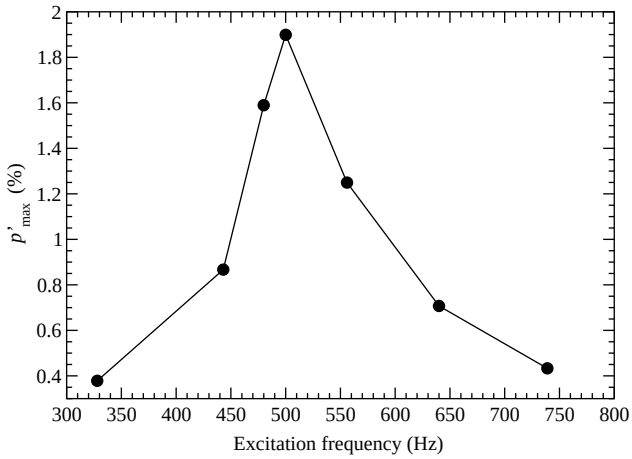

Figure 10. Variation of maximum unsteady pressure amplitude with excitation frequency.

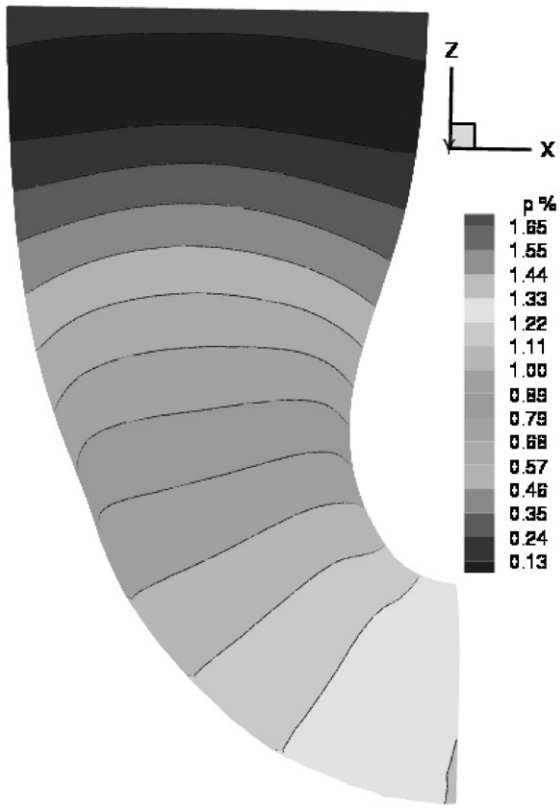

Figure 11. Unsteady pressure contours along the nozzle at 556 Hz.

Finally, it is instructive to observe the propagation of the unsteady pressure wave shape in the nozzle. An example is given in Figure 11 for the excitation case at 556 Hz. It is easily seen that the wave propagation is quasi-one-dimensional (quasi-1-D), with the wave aligning itself normal to the walls as it propagates downstream. An alternative way of looking at the pressure wave is to consider the maximum values along a surface line

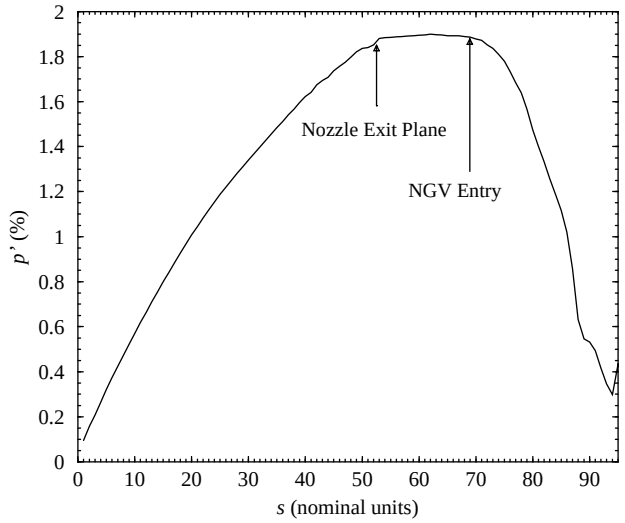

Figure 12. Variation of maximum pressure amplitude along nozzle at 500 Hz.

between the two boundaries of the computational domain. Such a plot is given in Figure 12 from which it is seen that the amplitude of the unsteady pressure grows steadily until the nozzle exit. The amplitude remains constant until the NGV entry and then decreases rapidly as the pressure drops with flow acceleration. The fact that the maximum unsteady pressure occurs at the nozzle exit may be considered to be detrimental to the structure since this area has high displacements for all "flap" type modes.

7. "CLOSED SYSTEM" CALCULATIONS

The calculations of the previous section effectively assume that the backward running waves escape from the upper boundary and that interactions with the combustion area and further reflections from the upper surface of the combustor are ignored. In the closed system calculations, the backward running waves are reflected back from the top of the combustor and added to the inlet pressure perturbation with a phase lag that is determined from the distance travelled at the speed of sound. Any interaction with the combustion area is ignored.

At the computational boundary, it is necessary to identify the forward and backward running waves, a task that is greatly simplified by the quasi-1-D nature of the flow (Figure 11). A typical example of such wave splitting is shown in Figure 13 for an inlet perturbation frequency of 580 Hz. Five different unsteady pressure quantities are plotted at a typical point on the upper boundary of the computational domain for a relatively short time interval. The solid line represents the actual value of the unsteady pressure, p, which is obtained through the summation of a number of different waves. The combustion disturbance, shown in dotted line, is represented by the applied inlet perturbation, p_f, with 0·3% zero-to-peak constant amplitude. The long dashed line is the identified backward running wave, p_b, which remains almost zero for the first 0.001 s, the time it takes the wave to travel the length of the nozzle and reflect back again. The dashed line, marked p_r, indicates the returning backward running wave which has been reflected from the top of the combustor. For closed system calculations, the applied inlet perturbation, labelled p_i, is the sum of p_f and p_r, while the actual unsteady pressure p is given by

$$p = p_r + p_f + p_b. \tag{2}$$

Figure 13 shows that, during the initial transient, both the total perturbation p_i and the actual pressure p grow because of the effect of the reflected wave p_r. However, as shown in Figure 14, a periodic state is reached soon after, the actual peak-to-peak values depending on phase differences and the excitation frequency of the applied inlet perturbation p_f.

The unsteady pressure shape inside the nozzle is shown in Figure 15 for both the open and closed system calculations for an excitation frequency of 566 Hz. Although the amplitude is higher for the closed system, the shape remains the same and hence the correlation with the "flap" modes of vibration is maintained. Such a feature can also be seen from the unsteady pressure contours of Figure 16, where the results of the open and closed system computations are compared. In the latter case, it is seen that the quasi-1-D behaviour of the flow is preserved in spite of higher levels of unsteadiness.

Further computations were performed with different excitation frequencies in order to assess the variation of maximum unsteady pressure amplitude with frequency. The results are plotted in Figure 17, where the corresponding open system curve is also been included.

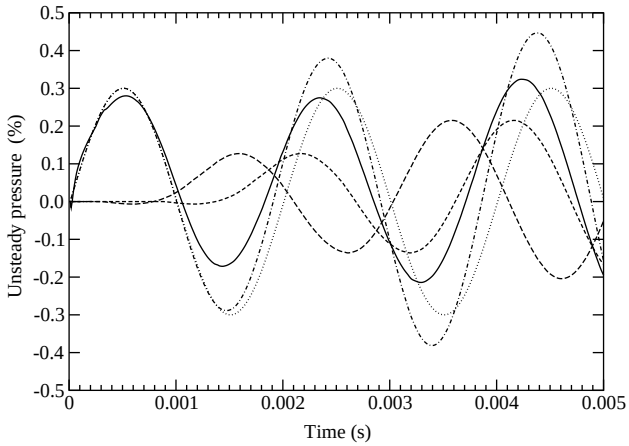

Figure 13. Wave decomposition at the inlet of the computational domain at 580 Hz: —, p; ...., p_f; - - -, p_r; – – –, p_b; – . – . –, p_i.

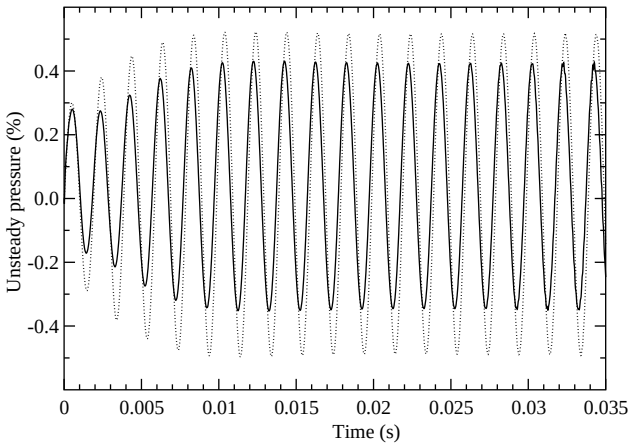

Figure 14. Actual and input unsteady pressures at the inlet of the computational domain at 580 Hz: —, p; ...., p_i.

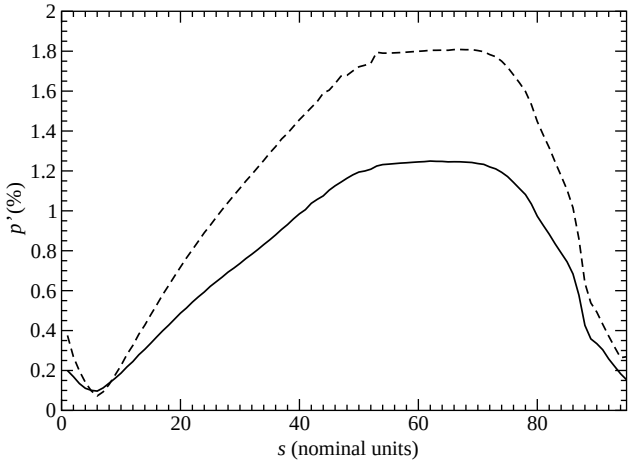

Figure 15. Variation of maximum amplitude along nozzle at 500 Hz: —, open system; - - - closed system.

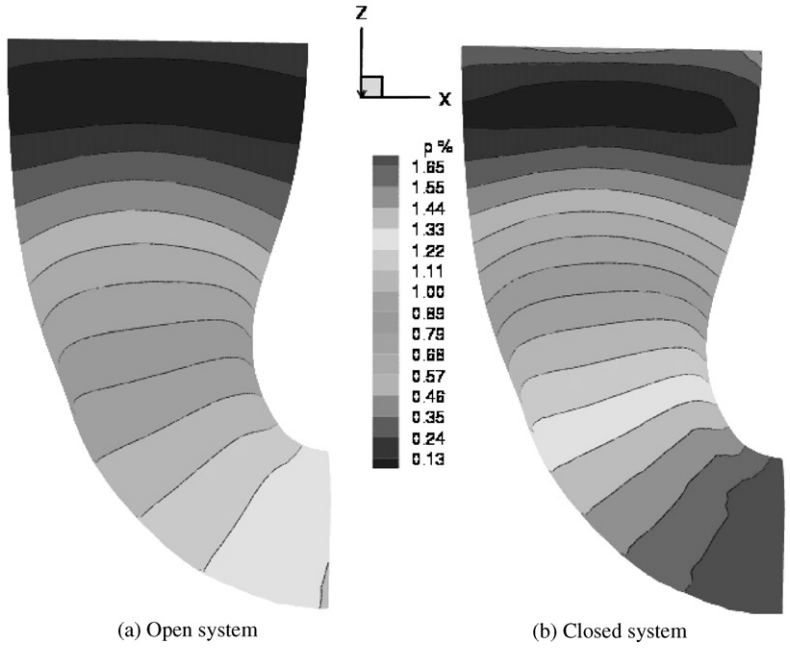

Figure 16. Unsteady pressure along the nozzle at 556 Hz.

Both curves show the same trend, though the peak occurs slightly earlier for the open system.

8. CONCLUDING REMARKS

From this study, the following may be concluded.

(i) A very simple combustion oscillation model has allowed to couple structural response and unsteady pressure variations. The investigation has shown that a shape

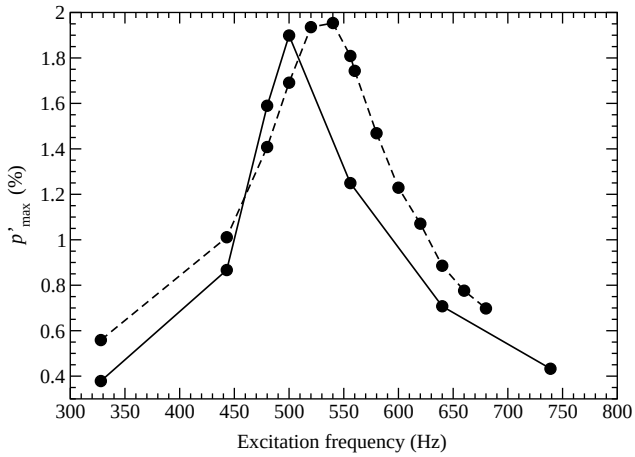

Figure 17. Variation of maximum unsteady pressure amplitude with excitation frequency: —, open - - -, closed systems.

match between the structural modes and the unsteady pressure distribution may lead to failure if the frequency of the perturbation also coincides with that of a structural mode.

(ii) More specifically, there is a distinct correlation between the flap modes of the discharge nozzle and the unsteady pressure shape arising from the disturbance created by the combustion process. On the other hand, the flex modes are unlikely to be excited by the unsteady pressure waves.

(iii) The maximum unsteady pressure amplitude is frequency dependent and a distinct peak, identified at around 550 Hz, is well within the experimentally observed high response range. Such a finding indicates the possibility of an acoustic resonance in the nozzle volume.

(iv) The trends above occur for both the open and closed systems, though maximum response is higher for the latter and occurs earlier for the former. The coexistence of these two factors, i.e., the match between the structural modes and the unsteady excitation, and the inherent unsteady pressure amplitude growth, increases the likelihood of very high vibration response for certain frequency ranges.

ACKNOWLEDGEMENTS

The authors would like to thank Rolls-Royce plc for both sponsoring this work and allowing its publication. They gratefully acknowledge the contribution of Dr C. Robinson for generating some of the results and of Dr K. Y. Sanliturk for his FE modelling. They also thank their colleagues at Rolls-Royce, Messrs C. Freeman and R. S. Wareing, and Dr I. K. Jennions, for many useful discussions.

REFERENCES

ALLEMANG, R. J. & BROWN, D. L. 1982 A correlation coefficient for modal vector analysis. In *Proceedings of the 1st International Modal Analysis Conference*, pp. 110–116, Orlando, FL, U.S.A.

BIRKBY, P., CANT, R. S., DAWES, W. N., DEMARGNE, A. A. J., DHANASEKARAN, P. C., KELLAR, W. P., RYCROFT, N. C., SAVILL, A. M., EGGELS, R. L. G. M. & JENNIONS I. K.

2000 CFD analysis of a complete industrial lean premixed gas turbine combustor. ASME Paper 2000-GT-0131.

Brookes, S. J., Cant, R. S., Dowling, A. P. 1999 Modelling combustion instabilities using computational fluid dynamics. ASME Paper 99-GT-112.

Brookes, S. J., Cant, R. S., Dupere I. D. J. & Dowling, A. P. 2000 Computational modelling of self-excited combustion instabilities. ASME Paper 2000-GT-104.

Hubbard, S. & Dowling, A. P. 2000 Acoustic resonances of an industrial gas turbine combustion system. In *Proceedings ASME TURBOEXPO 2000*, pp. 8–11, Munich, Germany. ASME Paper 2000-GT-94.

Newmark N. M., 1959 A method for the computation of structural dynamics. *Proceeding of the ASCE* EM3 85 76–94.

Sayma, A. I., Vahdati, M. & Imregun, M. 2000*a* Multi-stage whole-annulus forced response predictions using an integrated non-linear analysis technique — Part I: Numerical Model. *Journal of Fluids and Structures* **14,** 87–101.

Sayma, A. I., Vahdati, M., Sbardella, L. & Imregun, M. 2000*b* Modelling of 3D viscous compressible turbomachinery flows using unstructured hybrid grids. *AIAA Journal* **38,** 945–954.

Sbardella, L., Sayma, A. I. & Imregun, M. 2000 Semi-structured meshes for axial turbomachinery blades. *International Journal of Numerical Methods in Fluids* **32,** 569–584.

Smith, C. E. & Leonard, A. D. 1997 CFD Modelling of combustion instability in premixed axisymmetric combustors. ASME Paper 97-GT-305.

Vahdati, M. & Imregun, M. 1996 A non-linear integrated aeroelasticity analysis of a fan blade using unstructured dynamic meshes. *Institution of Mechanical Engineers, Journal of Mechanical Engineering Science — Part C* **210,** 549–563.

Zhu, M., Dowling, A. P. & Bray, K. N. C. 2000 Self-excited oscillations in combustors with spray atomisers. ASME Paper 2000-GT-108.